Article

Discovery Medicine 2023; 35(179): 1052–1063
https://doi.org/10.24976/Discov.Med.202335179.101

Application of Routine Echocardiography Combined with Contrast-Enhanced Echocardiography in the Diagnosis of Endomyocardial Fibrosis

Bijun Wu[1,2], Yaolin Yang[3], Ping Zhao[4,*]

[1]Guangzhou University of Chinese Medicine, 510006 Guangzhou, Guangdong, China
[2]Ultrasonic Department, Guangdong Second Provincial General Hospital, 510317 Guangzhou, Guangdong, China
[3]Department of Cardiology, Guangdong Second Provincial General Hospital, 510317 Guangzhou, Guangdong, China
[4]Ultrasonic Department, The First Affiliated Hospital of Guangzhou University of Chinese Medicine, 510405 Guangzhou, Guangdong, China
*Correspondence: zhaosiping@126.com (Ping Zhao)
Published: 1 December 2023

Background: In China, endomyocardial fibrosis (EMF) is a type of restrictive cardiomyopathy that is rare and easy to be misdiagnosed. Our aim was to examine the value of routine echocardiography (RE) combined with contrast-enhanced echocardiography (CEE) in EMF diagnosis.

Methods: We studied 16 EMF patients retrospectively, from 2012 to 2022. All patients underwent RE, from which 11 underwent CEE. We divided the patients into three groups: biventricular EMF (Bi-EMF), right ventricular EMF (RV-EMF), and left ventricular EMF (LV-EMF) based on different lesion locations. We also analyzed the clinical and conventional ultrasound characteristics of the three groups of patients and examined the ventricle opacification (VO) and myocardial contrast echocardiography (MCE) characteristics of patients who underwent CEE.

Results: All patients with EMF subtypes had the following ultrasound findings: apical occlusion on one or both sides, corresponding atrial dilatation, atrioventricular valve regurgitation in varying degrees, and cardiac diastolic dysfunction. Of the subjects, 69% had apical thrombus calcification and 81% had mild pericardial effusion. RV-EMF patients had statistically significant right atrial enlargement compared with the other two groups ($p < 0.05$), moderate or severe tricuspid regurgitation, and inferior vena cava (IVC) dilation. LV-EMF patients had statistically significant left atrial enlargement compared with the other two groups ($p < 0.05$), elevated pulmonary artery systolic pressure (PASP), and 60% of LV-EMF patients had moderate or severe mitral regurgitation. Bi-EMF patients had bilateral atrial enlargement, an IVC collapsibility index <50%, and elevated PASP. CEE was performed in 11 patients, whose ventricle opacification showed no contrast filling in the apical occluded area and the heart chambers presented the "mushroom sign" during diastole. Their myocardial contrast echocardiography (MCE) showed delayed perfusion in the thickened fibrotic endomyocardium (TFE) of the apical and subvalvular regions and perfusion defect in the apical thrombus. The number and location of thrombus determined by the MCE combined with RE were the same as those detected by cardiac magnetic resonance imaging (CMR). MCE shows that the position and range of TFE are similar to CMR.

Conclusions: EMF has characteristic RE presentation, and different EMF subtypes have unique characteristics. CEE can better display heart structure, ventricular wall motion, and tissue perfusion compared to RE. A combination of RE and CEE can make the EMF diagnosis more accurate, thereby allowing early treatment for EMF patients.

Keywords: endomyocardial fibrosis; restrictive cardiomyopathy; contrast echocardiography; cardiac magnetic resonance imaging

Introduction

Endomyocardial fibrosis (EMF) is an overlooked endemic restrictive cardiomyopathy that is prevalent in tropical and subtropical developing countries and was first reported in Uganda by Davies in 1948 [1]. EMF is commonly found in central Africa but is seldom seen in China. The highest incidence of this condition is observed in the regions of Guangxi, Guangdong, and Guizhou. Although there is still a lack of knowledge on the etiology and pathogenesis of EMF, it is believed to be caused by the joint effects of parasitic worm infection, poverty, malnutrition, and genetic susceptibility. This stimulates inflammation and immunomodulation, resulting in endomyocardial fibrosis that mainly involves the apical and subvalvular regions in one or two ventricles. EMF is classified into three forms based on lesion site, namely biventricular EMF (Bi-EMF), left ventricular EMF (LV-EMF), and right ventricular EMF (RV-EMF) [2]. Most EMF patients have normal ventricular systolic function. Diastolic insufficiency is the cause of severe heart failure (HF) in patients [3,4]. Currently, there is no effective treatment, but surgical resection of the thickened endocardium and simultaneous valve repair or replacement

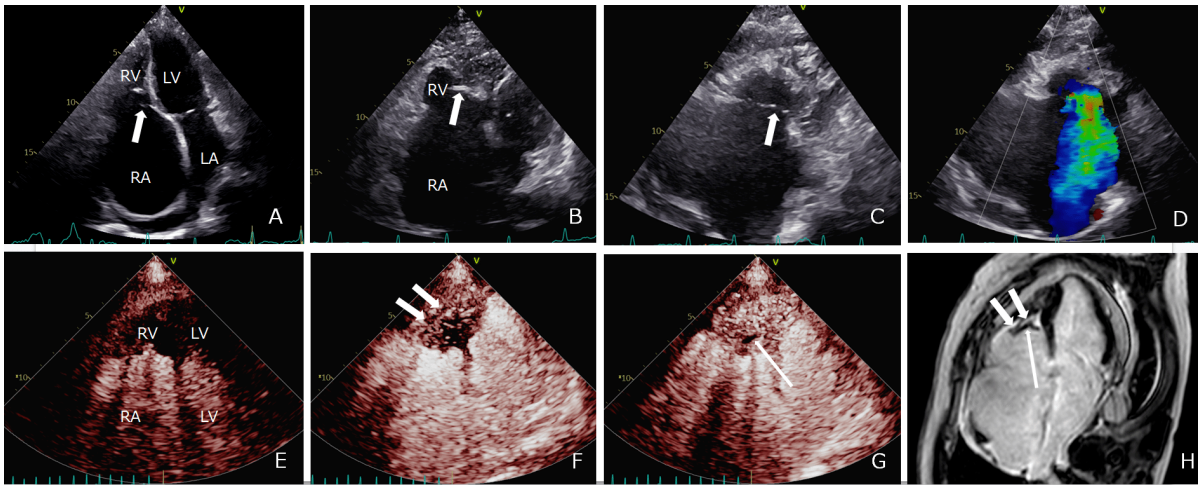

Fig. 1. RV-EMF patient. (A) Apical 4-chamber view during systole showed significant RA enlargement and downward traction on tricuspid valve septal leaflet (arrow). (B) RV shrinkage and deformation, RV apical occlusion, and thrombus calcification (arrow). (C,D) Right ventricular inflow tract view shows the fissure when tricuspid valve is close (arrow), and severe TR. (E–G) They are MCE images after high-energy pulse flash, which are the first cardiac cycle, the third cardiac cycle, and the plateau phase, respectively. Perfusion in the myocardium of the occlusion site was normal (short arrows), perfusion in the TFE was delayed, and perfusion in the uncalcified thrombus was absent (long arrow). (H) CMR late gadolinium enhancement TFE showed typical "V sign" (short arrows). The black area was the thrombus (long arrow). RV, right ventricle; RA, right atrium; TR, tricuspid regurgitation; MCE, myocardial contrast echocardiography; TFE, thickened fibrotic endomyocardium; CMR, cardiac magnetic resonance imaging; LV, left ventricle; LA, left atrium; EMF, endomyocardial fibrosis; RV-EMF, right ventricular endomyocardial fibrosis.

can improve survival rate compared with drug treatment [5,6]. This may be the only option to improve EMF prognosis. However, advanced EMF patients with severe HF and malignant signs are unsuitable for surgery. Hence, prompt diagnosis of EMF is extremely important [3].

Endomyocardial biopsy is the gold standard for EMF diagnosis, but the risk of injury is high. Also, endocardial fibrosis, mural thrombus organization, and calcification cause the biopsy success rate to be low [7]. Cardiac magnetic resonance imaging (CMR) can provide detailed anatomical, morphological, and functional information on the heart. Late gadolinium enhancement can be used to evaluate the presence of myocardial inflammation, injury, and fibrosis, and it is the standard for non-invasive EMF diagnosis and fibrosis evaluation [8–11].

However, magnetic resonance imaging (MRI) examinations are expensive and have high technical requirements; only large hospitals possess MRI equipment. Hence, CMR cannot be used for routine examination. Echocardiography is widely used in clinical practice and it is the first-line method for EMF evaluation [12–14]. However, EMF is rare and there is no known characteristic clinical presentation of EMF, making it easy to be misdiagnosed by inexperienced ultrasound physicians. In this study, we analyzed the echocardiography results of 16 clinically confirmed EMF patients to examine the role of routine echocardiography (RE) combined with contrast-enhanced echocardiography (CEE) in diagnosis, in order to achieve immediate treatment and improve the quality of life and prognosis of patients.

Data and Methods

Study Participants

After the study was approved by the institutional review board of Guangdong Second Provincial General Hospital, data from January 2012 to August 2022 were collected from the hospital's case database in a retrospective mode. The information included 16 EMF cases confirmed by endomyocardial biopsy and/or CMR. There were nine males and seven females, and their ages ranged from 48 to 77 (60 $\pm$ 8) years. Eleven subjects were from Guangdong province and five were from Guangxi province. The disease course ranged from three months to nine years. The main symptoms in all the patients were recurrent chest tightness and shortness of breath, which was accompanied by edema of both lower extremities in nine of them, jugular vein distension in four and cough accompanied by expectoration in two. The median eosinophil count for the individuals was $< 0.5 \times 10^9$ g/L. Coronary angiography results were all negative. Three subjects underwent endomyocardial biopsy and 13 underwent CMR. Sixteen patients underwent RE, among which 11 went through CEE at the same time.

Equipment and Methods

All subjects underwent a complete echocardiography evaluation using iE33 imaging system (Philips, Andover, MA, USA), 7c imaging system (Philips, Andover, MA, USA) or vivid E95 scanner (GE Vingmed Ultrasound, Horten, Norway), whose probe frequencies were

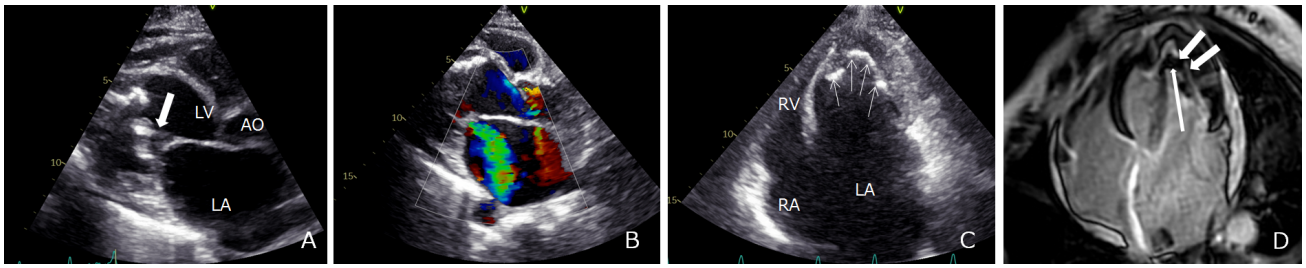

Fig. 2. LV-EMF patient. (A,B) LV long axis view shows mitral valve chordae tendineae thickening and echo enhancement (arrow), papillary muscle fusion to TFE and thrombus, valves being pulled down during systole and mild MR. (C) Apical 4-chamber view during systole shows significant LA enlargement, LV apical occlusion, and thrombus calcification (arrows). (D) CMR late gadolinium enhancement TFE shows typical "V sign" (short arrows). The upper black area in TFE represents the thrombus (long arrow). LV, left ventricle; LA, left atrium; MR, mitral regurgitation; AO, aorta.

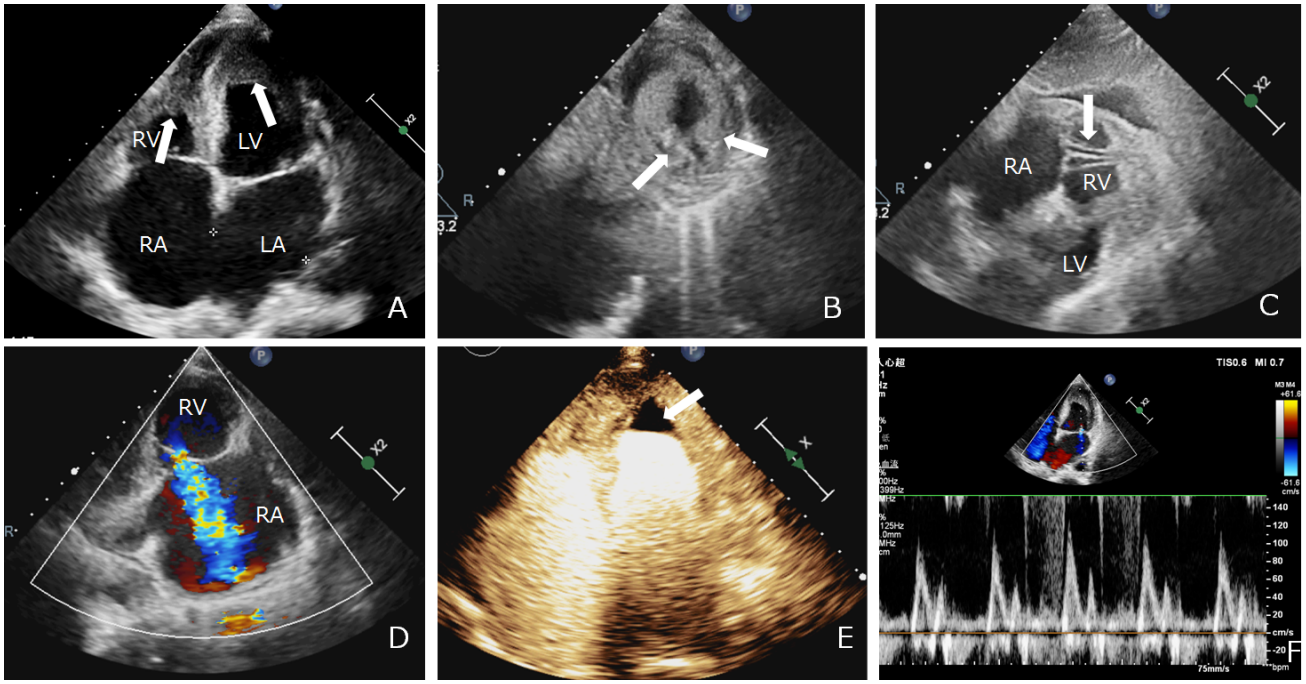

Fig. 3. Bi-EMF patient. (A) Apical 4-chamber view during systole shows bilateral atrial enlargement and bilateral ventricle apical occlusion (arrows). (B) LV short-axis view shows mitral valve papillary muscle fusion to TFE and thrombus (arrows). (C,D) Subxiphoid 4-chamber view shows tricuspid valve chordae tendineae thickening and echo enhancement (arrow), papillary muscle fusion to TFE and thrombus, valves pulled down during systole and moderate-severe TR. (E) In MCE plateau stage, perfusion is absent in the apical thrombus (arrow). (F) Restrictive mitral valve blood flow frequency spectrum of EMF patient: E/A >2, DT <140 ms. Bi-EMF, biventricular endomyocardial fibrosis; E, peak E-wave velocity; A, peak A-wave velocity; D, E-wave deceleration time.

2.0–3.5 MHz, 1.6–3.2 MHz, and 1.4–4.6 MHz respectively. Echocardiography parameters were analyzed according to the American Society of Echocardiography guidelines, including Doppler measurements, M mode and two-dimensional (2D) imaging [15]. The biplane disk method, a modified Simpson's technique, was used to calculate the left ventricular end-diastolic volume (LVEDV) and the left ventricular ejection fraction (LVEF). The left ventricular end-diastolic volume index (LVEDVI) can be obtained from the fraction result LVEDV/body surface area (BSA). The left atrial volume (LAV) was measured from apical 4-chamber and 2-chamber views using the biplane disk method at ventricular end-systole (when the left atrial diameter is at its maximum value). The left atrial volume index (LAVI) can be calculated as LAV/BSA. The right ventricular end-systolic area (RVESA) and right ventricular end-diastolic area (RVEDA) were obtained from the right ventricular focused apical 4-chamber view. The right ventricular end-diastolic area index (RVEDAI) can be acquired from the division RVEDA/BSA. The formula for right ventricular fractional area change (RVFAC) is: (RVEDA - RVESA)/RVEDA $\times$ 100. The right atrial volume (RAV)

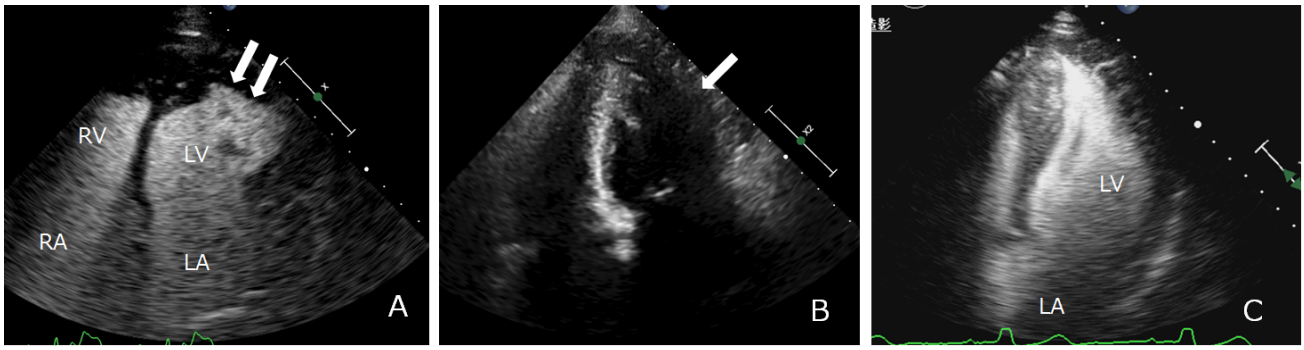

Fig. 4. VO in EMF patient and APHCM patient. (A,B) EMF patient. In apical 4-chamber view, there was severe endocardial calcification (arrow), chambers were not clearly displayed, and chambers were clearly displayed on VO as "mushroom sign". (C) APHCM patient. Ventricle opacification during diastole showed "spade-shape". VO, ventricle opacification; APHCM, apical hypertrophic cardiomyopathy.

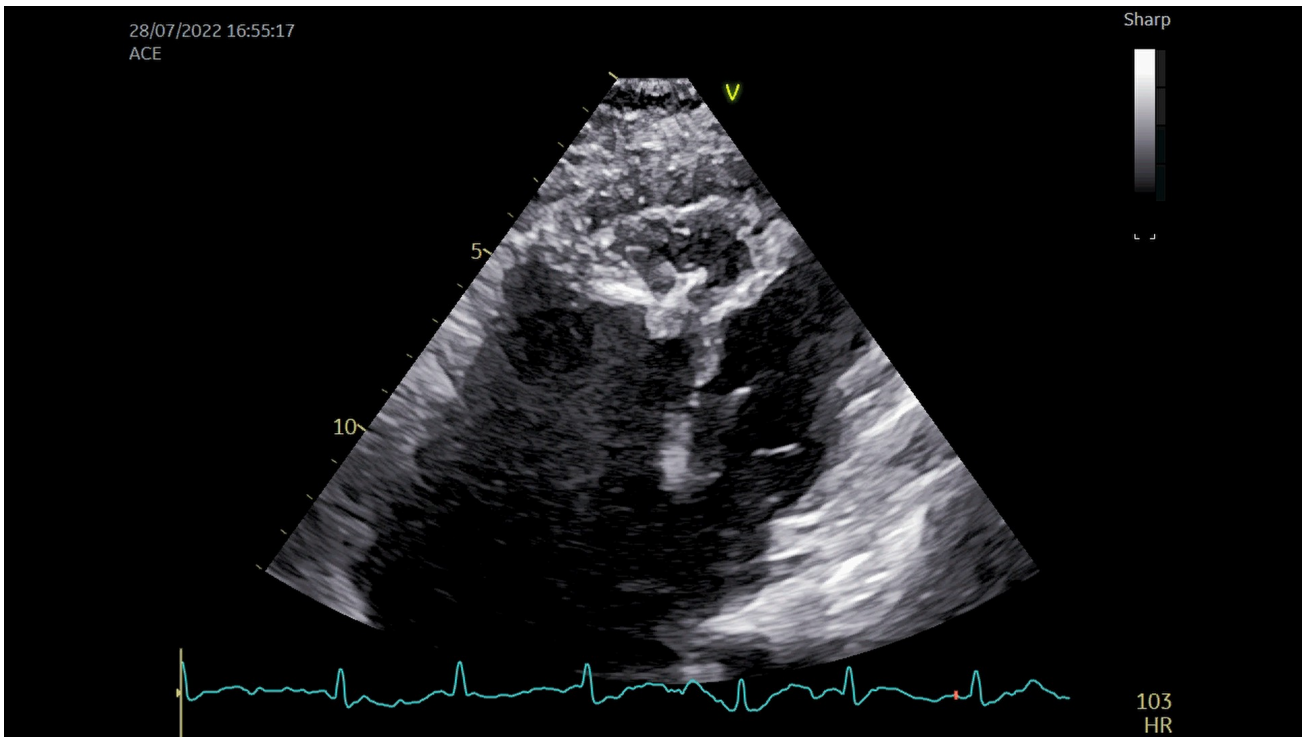

Video 1. The ventricular base showed excessive motion compared with the apex. HR: heart rate. The embedded movie may also be viewed at https://doi.org/10.24976/Discov.Med.202335179.101.

was measured from the apical 4-chamber view using the biplane disk method at ventricular end-systole (when the right atrial diameter is at its maximum value). The right atrial volume index (RAVI) is RAV/BSA. The pulmonary artery systolic pressure (PASP) was calculated at peak systolic blood flow using Bernoulli's equation. The right atrium (RA) pressure was derived based on the inferior vena cava diameter and its respiratory change. Mitral and tricuspid diastolic function measurements included the following: sinus rhythm, mitral and tricuspid diastolic phase peak E-wave velocity (E), peak A-wave velocity (A), and E-wave deceleration time (DT). Base on this data, the E/A ratio was calculated. For atrial fibrillation, mitral and tricuspid E, early diastolic mitral annular motion velocity (e') at the interventricular septum and lateral wall of the mitral annulus and e' at the anterior tricuspid annulus were measured; then E/e' was calculated. The severity of mitral and tricuspid regurgitation was graded using an integrated and semi-quantitative approach as mild, moderate, or severe [16].

CEE was performed as follows: 5 mL of 0.9% sodium chloride solution was added to the contrast agent SonoVue and shaken to form a microbubble suspension and 2.5 mL of the mix was diluted with 12.5 mL of 0.9% sodium chloride solution. Then a 20 G intravenous needle was used for injection at a uniform speed for 2 minutes in the left cubital vein. Ventricle opacification (VO): The VO imaging

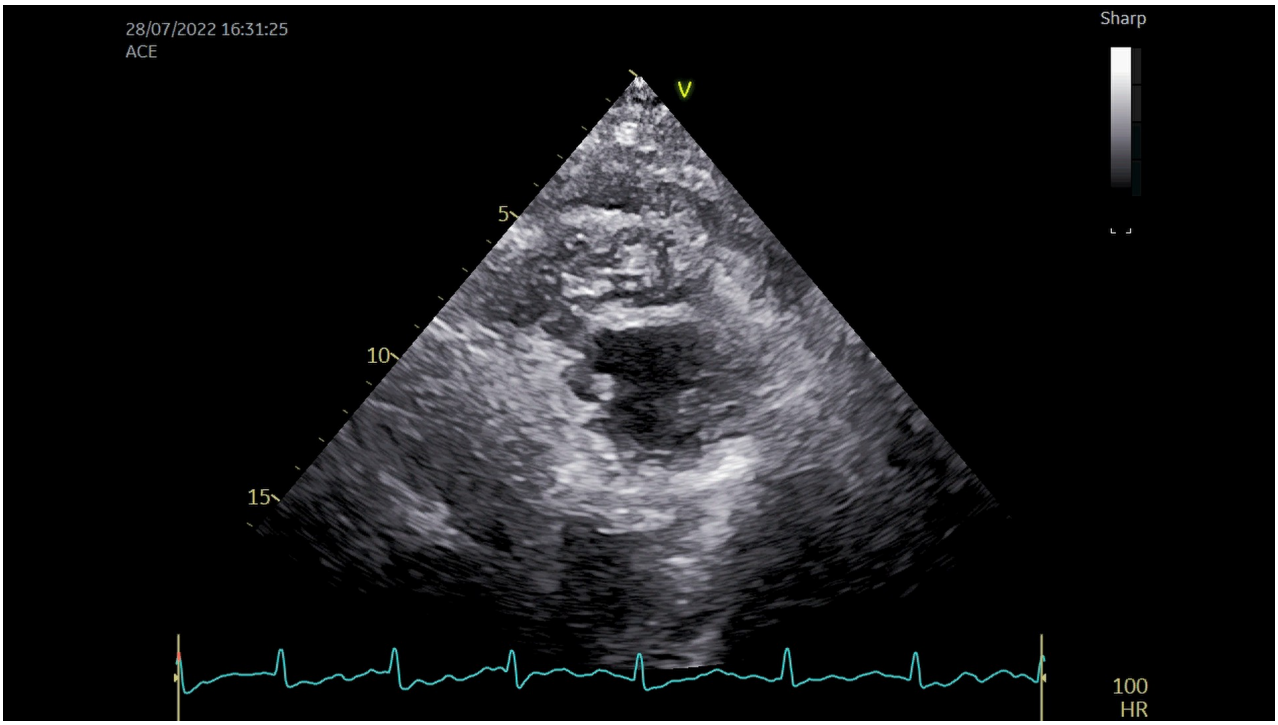

Video 2. There was no significant decrease in myocardial motion at the occlusion site. The embedded movie may also be viewed at https://doi.org/10.24976/Discov.Med.202335179.101.

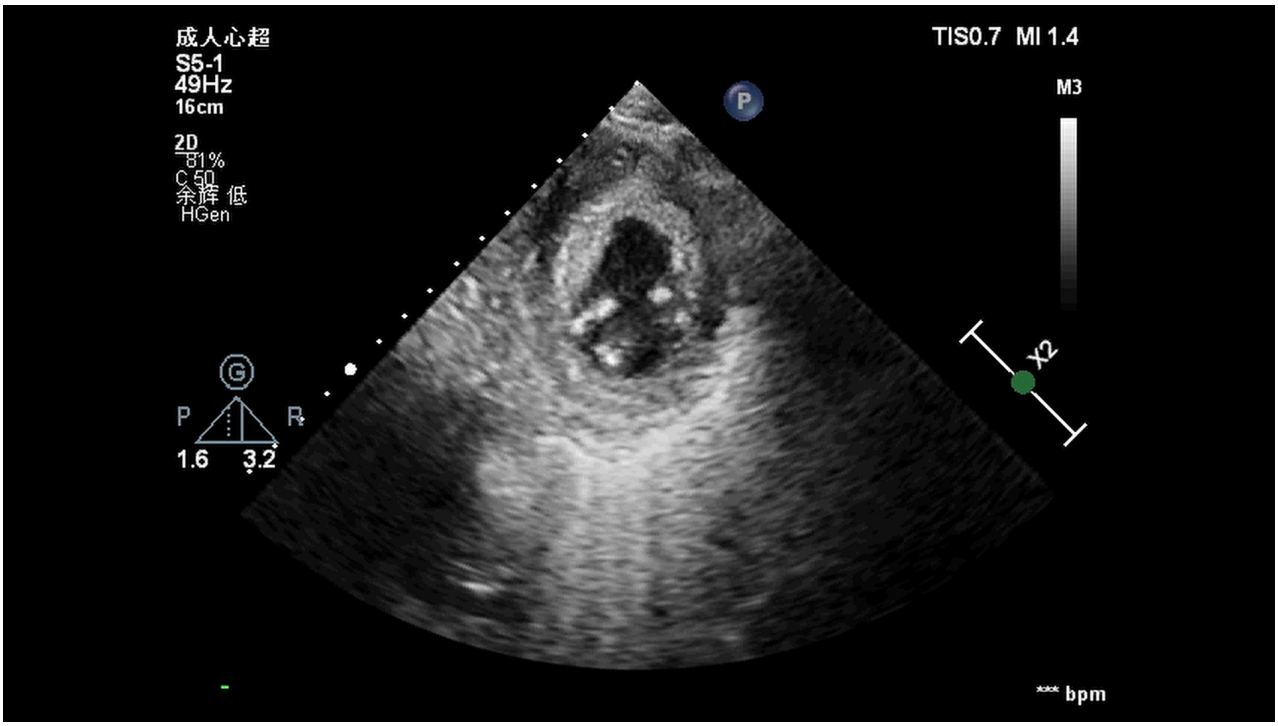

Video 3. LV short-axis view showed mitral valve papillary muscle fusion to TFE and thrombus. The embedded movie may also be viewed at https://doi.org/10.24976/Discov.Med.202335179.101.

mode was selected. Apical 4-chamber, 3-chamber, and 2-chamber and right ventricular inflow tract images were acquired and stored. Five cardiac cycles were stored for each view.

Myocardial contrast echocardiography (MCE) was performed as follows: the instrument was switched to low mechanical index real-time imaging mode, MI-0.08. Once the intramyocardial contrast agent was stable, a high-energy

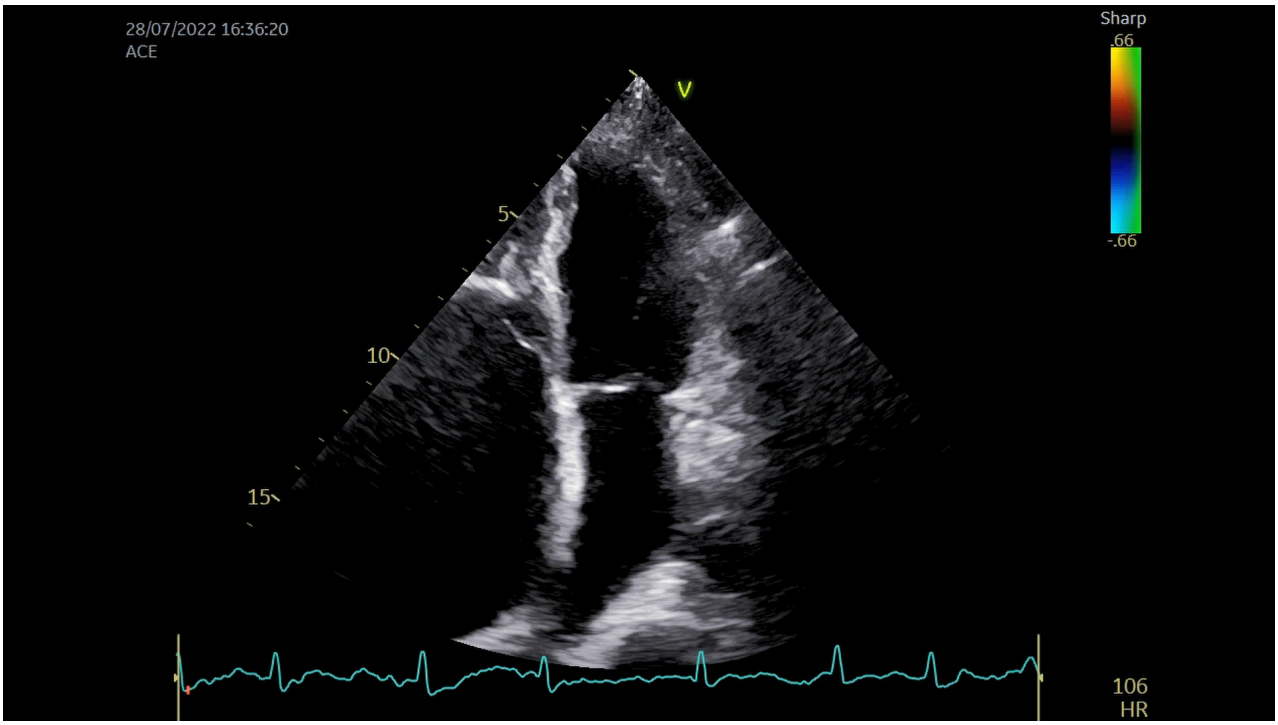

Video 4. Apical 4-chamber view showed significant RA enlargement and downward traction on tricuspid valve septal leaflet. The embedded movie may also be viewed at https://doi.org/10.24976/Discov.Med.202335179.101.

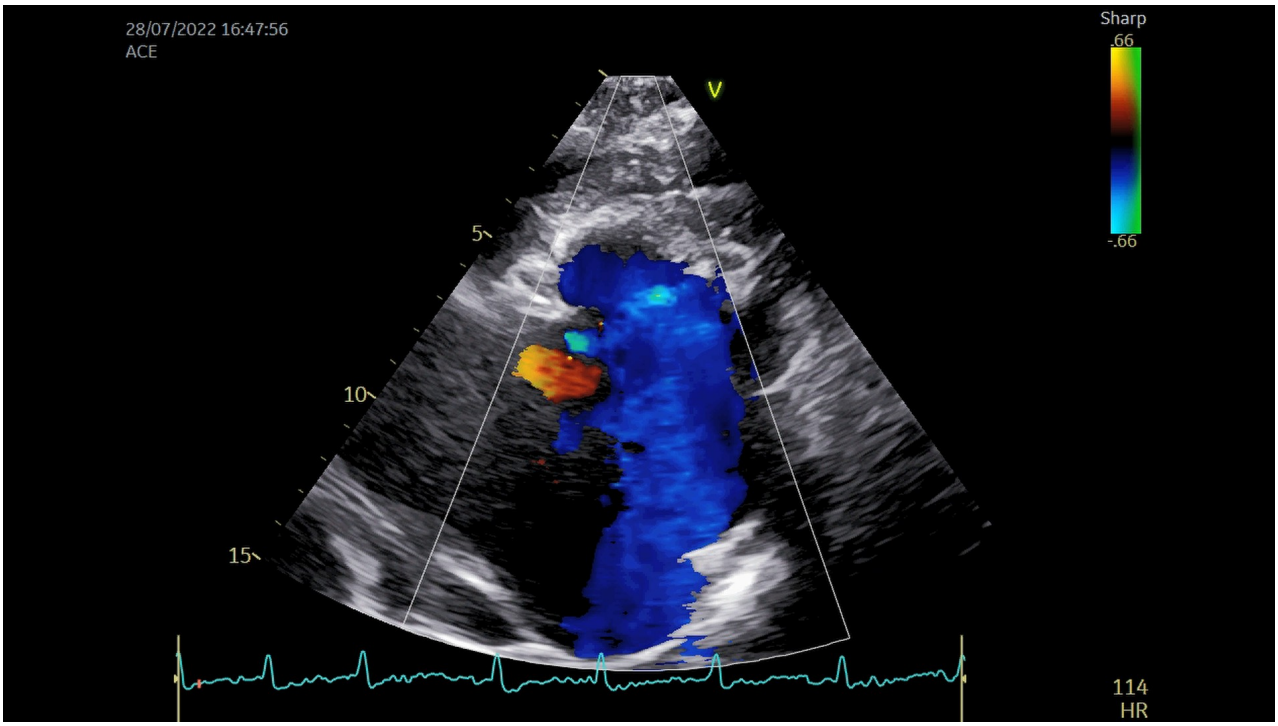

Video 5. Color doppler imaging showed severe TR. The embedded movie may also be viewed at https://doi.org/10.24976/Discov.Med.202335179.101.

pulse flash (15 frames/s) was triggered to disrupt the microbubbles in intramyocardial angiography, and the myocardial microbubble reperfusion imaging was acquired.

Statistical Analysis

SPSS 21.0 software (IBM, Chicago, IL, USA) was used for statistical analysis. Normally distributed quantitative data were expressed as mean ± standard devia-

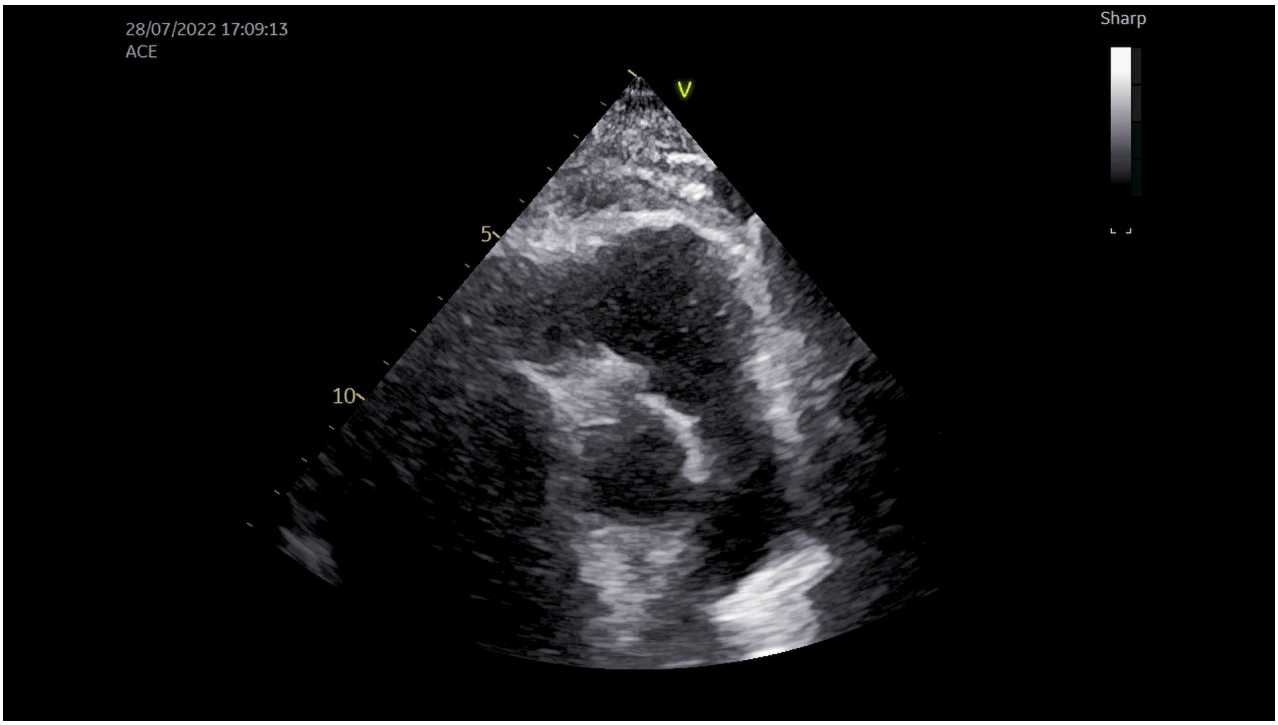

Video 6. Right ventricular outflow tract view showed outflow tract dilatation. The embedded movie may also be viewed at https://doi.org/10.24976/Discov.Med.202335179.101.

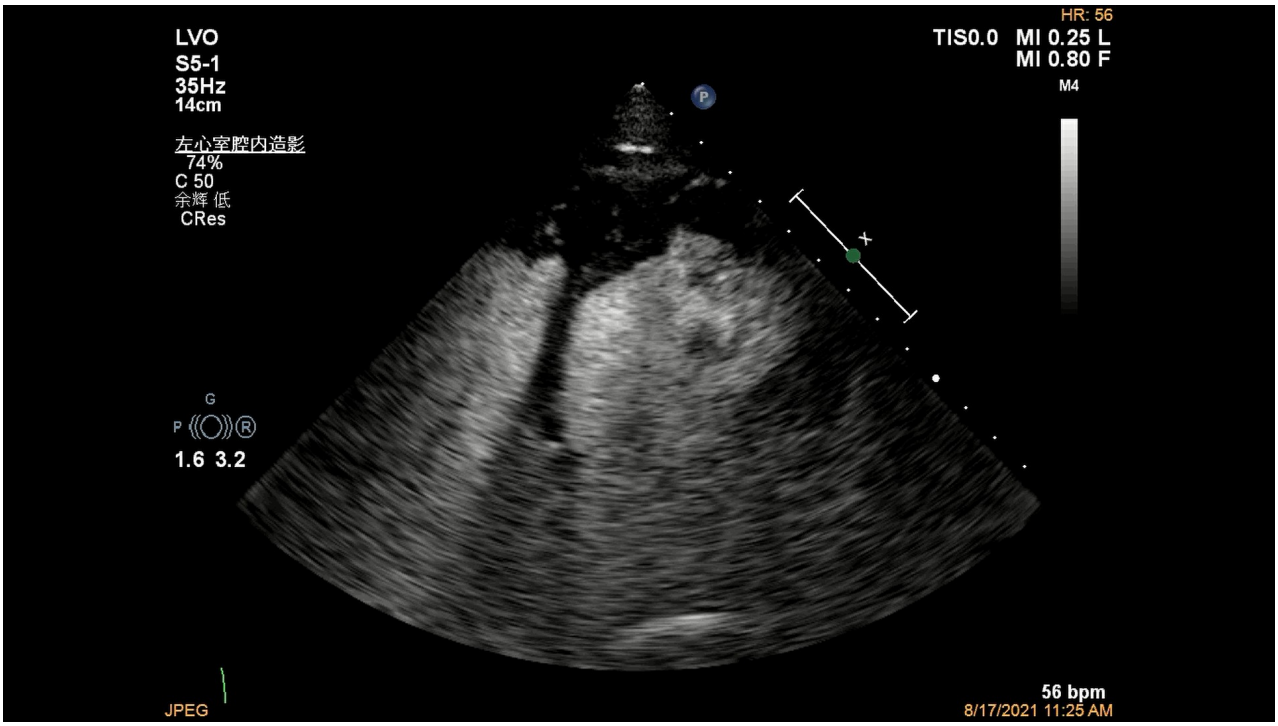

Video 7. VO (Ventricle opacification): Cardiac cavity clearly displayed in EMF patients with severe calcification. The embedded movie may also be viewed at https://doi.org/10.24976/Discov.Med.202335179.101.

tion. One-way ANOVA was used for inter-group comparison while the least significant difference (LSD) test was used for pair-wise comparison. Qualitative data were expressed as number of patients and percentages, and the Fisher-Freeman-Halton Exact Test was utilized for inter-group comparison. $p < 0.05$ was considered to indicate a statistically significant difference.

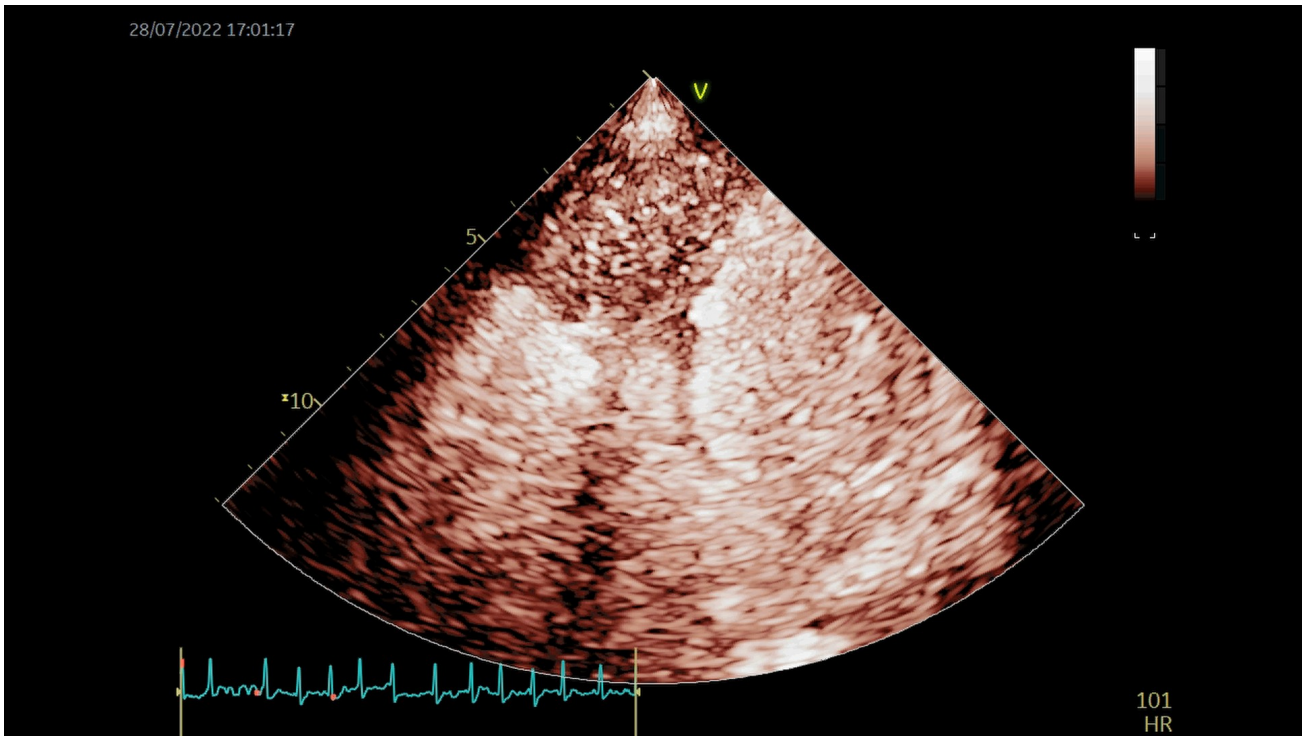

Video 8. MCE: Perfusion in myocardium of the occlusion site was normal, perfusion in TFE was delayed, and perfusion in the uncalcified thrombus was absent. The embedded movie may also be viewed at https://doi.org/10.24976/Discov.Med.202335179.101.

Results

Out of the 16 patients, only one had an echocardiography result of EMF at the first hospitalization, whereas the others were treated in at least two hospitals and underwent at least two echocardiography examinations. The initial ultrasound diagnoses of these patients are shown in Table 1. Ultimately, 7 (44%), 4 (25%), and 5 (31%) patients were diagnosed with Bi-EMF, RV-EMF, and LV-EMF, respectively. Fifteen patients were grouped, taking into account their symptoms, inside class III/IV, according to the New York Heart Association (NYHA) functional class. One patient with LV-EMF was categorized inside NYHA functional class II. Electrocardiography showed that 6 (38%) patients had atrial fibrillation, of which the right ventricular form is the most common; 5 (31%) had ST-T changes; 3 (19%) had frequent premature atrial contractions; 2 (13%) had paroxysmal atrial tachycardia; one had paroxysmal ventricular tachycardia; and two had complete right bundle branch block. There were no statistically significant differences in age, gender, or surface area between different EMT subtypes (all $p < 0.05$) (Table 2).

Ultrasound results common to all EMF subtypes were as follows: (1) Unilateral or bilateral ventricular apical subvalvular thickening, apical occlusion, apical thrombus calcification in most patients (69%), decreased ventricular long axis, normal or increased transverse diameter and corresponding atrial dilation (Fig. 1A,B; Fig. 2A; Fig. 3A), ventricular base showing excessive motion compared with the apex (Video 1), no significant decrease in myocardial motion at the occlusion site (Video 2), mild pericardial effusion in 81% of patients (Fig. 1A; Fig. 2A). (2) Tricuspid valve and/or mitral valve chordae tendineae thickening and echo enhancement. Papillary muscle fused to thickened fibrotic endomyocardium (TFE) and thrombus (Fig. 3B; Video 3). Valves were unable to close properly and pulled down during systole (Fig. 1C; Fig. 2A; Fig. 3C; Video 4). The degree of regurgitation varies (Fig. 1D; Fig. 2B; Fig. 3D; Video 5). (3) Systolic function was normal, diastolic dysfunction was present, 9 sinus rhythm patients had restrictive diastolic dysfunction in the

Table 1. Initial ultrasound diagnosis of the endomyocardial fibrosis patients.

Type	N	Ultrasound diagnosis
Bi-EMF	3	Apical hypertrophic cardiomyopathy
	2	Coronary heart disease with apical thrombus
	1	Atrioventricular valve regurgitation
RV-EMF	1	Constrictive pericarditis
	2	Ebstein anomaly
	1	Right ventricular cardiomyopathy
LV-EMF	2	Apical hypertrophic cardiomyopathy
	2	Coronary heart disease with apical thrombus
	1	Mitral valve lesion

Bi-EMF, biventricular endomyocardial fibrosis; RV-EMF, right ventricular endomyocardial fibrosis; LV-EMF, left ventricular endomyocardial fibrosis.

Table 2. Clinical and routine echocardiography characteristics of endomyocardial fibrosis patients.

Parameter	All EMF (n = 16)	RV-EMF (n = 4)	LV-EMF (n = 5)	Bi-EMF (n = 7)	F-value/χ^2	p-value
Age (years)	60 ± 8	60 ± 8	62 ± 10	59 ± 8	0.145	0.866
Male (%)	9 (56%)	2 (50%)	3 (60%)	4 (57%)	0.350	1.000
Body surface area	1.63 ± 0.14	1.60 ± 0.15	1.65 ± 0.14	1.63 ± 0.16	0.134	0.876
Atrial fibrillation	6 (38%)	3 (75%)	1 (20%)	2 (28%)	2.953	0.344
NYHA class, III/IV	15 (94%)	4 (100%)	4 (80%)	7 (100%)	2.156	0.562
LVEF, %	61.75 ± 3.13	63.75 ± 3.10	60.00 ± 3.61	61.86 ± 2.41	1.765	0.210
LVEDVI (mL/m^2)	49.94 ± 6.03	46.00 ± 6.48	54.00 ± 6.28	49.29 ± 4.34	2.413	0.129
RVFAC, %	47.43 ± 6.72	43.25 ± 6.39	52.20 ± 5.97	46.42 ± 6.08	2.544	0.117
RVEDAI (cm^2/m^2)	11.06 ± 1.80	11.68 ± 2.11	10.52 ± 1.76	11.09 ± 1.83	0.422	0.664
LAVI (mL/m^2)	63.38 ± 28.83	29.00 ± 3.37	94.80 ± 23.15^a	60.57 ± 9.76^{bc}	22.985	0.001
RAVI (mL/m^2)	67.31 ± 36.02	118.50 ± 27.33	32.80 ± 5.12^a	62.71 ± 9.45^{bc}	37.414	0.001
PASP (mmHg)	47.50 ± 12.18	32.25 ± 1.71	54.80 ± 12.95^a	51.00 ± 6.63^b	8.835	0.004
Moderate or severe MR	5 (31%)	0	3 (60%)	2 (28%)	3.301	0.263
Moderate or severe TR	7 (44%)	4 (100%)	1 (20%)	2 (28%)	6.341	0.031
Apical thrombus calcification	11 (69%)	4 (100%)	3 (60%)	4 (57%)	2.279	0.407
Pericardial effusion	13 (81%)	4 (100%)	4 (80%)	5 (71%)	1.266	0.750

NYHA, New York Heart Association; LVEF, left ventricular ejection fraction; LVEDVI, left ventricular end-diastolic volume index; RVFAC, right ventricular fractional area change; RVEDAI, right ventricular end-diastolic area index; LAVI, left atrial volume index; RAVI, right atrial volume index; PASP, pulmonary artery systolic pressure. $^a p < 0.05$, LV-EMF vs RV-EMF; $^b p < 0.05$; Bi-EMF vs RV-EMF; $^c p < 0.05$ Bi-EMF vs LV-EMF.

involved ventricles, atrioventricular valve frequency spectrum showed restrictive filling pattern (Fig. 3F), E/A >2, DT <140 ms, E/e' of involved ventricles >11 in atrial fibrillation patients.

The RV-EMF ultrasound results were as follows: severe dilatation of the right atrium (RA) [RAVI was (118.50 ± 27.33 mL/m^2)], which was statistically significant compared with the other two groups ($p < 0.05$) (Table 2). The right ventricular outflow tract was normal or dilated (Video 6); the left atrium and ventricle were not enlarged; and the left cardiac function was normal. Moderate or severe tricuspid regurgitation (TR) was observed (3 patients had severe TR), and PASP was normal. Dilation of the inferior vena cava (IVC) was observed with a diameter >2.1 cm and a collapsibility index <50%.

The LV-EMF subsequent ultrasound results were: left atrial (LA) enlargement (LAVI was 94.80 ± 23.15 mL/m^2), which was statistically significant compared with the other two groups ($p < 0.05$) (Table 2), and normal or mildly enlarged RA (Fig. 2C). Moderate or severe mitral regurgitation (MR) (60%) was common. There was a mild to moderate increase in PASP (54.80 ± 12.95 mmHg). Four patients (80%) developed left ventricular (LV) restrictive diastolic dysfunction.

The Bi-EMF ultrasound results were as follows: bilateral atrial enlargement with a similar degree between the two atria. Apical thrombus calcifications were all located in the LV. Most patients had mild MR and TR. Four patients had moderate-severe MR or TR. There was a mild to moderate increase in PASP (51.00 ± 6.63 mmHg) and no statistically significant difference compared with the LV-EFT group ($p > 0.05$). IVC collapsibility index was <50%, and one patient presented IVC diameter >2.1 cm.

Eleven patients, including five cases of unclear diagnosis by RE and six cases of blood supply status of the apical occlusion, underwent CEE followed by CMR. Overall, five, three, and three patients had Bi-EMF, RV-EMF and LV-EMF, respectively. VO characteristics are that there is no contrast agent filling in apical occlusion areas and heart chambers show a "mushroom sign" during diastole [6] (Fig. 4A). Due to severe apical thrombus calcification in three patients, ventricles were not clear in RE (Fig. 4B) but heart chambers could be clearly seen in VO (Fig. 4A); excessive basal ventricular motion was easily observed (Video 7).

During MCE, the normal myocardium of the involved area was perfused simultaneously with the same intensity as that in the uninvolved area; as a result, the myocardium did not get thinner. The perfusion in the thickened fibrotic endomyocardium was slow, specifically, in the apical and subvalvular regions. The perfusion from the outside to the inside was gradual (Fig. 1E,F; Video 8). At the plateau stage, the TFE showed the same perfusion intensity as the normal myocardium (Fig. 1G; Fig. 3E). Uncalcified thrombus did not show a contrast agent perfusion from Flash to plateau, presenting as a dark area (Fig. 1G; Fig. 3E). CMR late gadolinium enhancement of TFE showed a continuous region that usually extended from the subvalvular zone to the apex, presenting a "V sign", thrombus and calcification were the dark regions (Fig. 1H; Fig. 2D). CMR detected seven cases of left ventricular thrombus and six cases of

right ventricular thrombus. The number and location of thrombus determined by the MCE combined with RE were the same as those detected by CMR. The MCE and CMR displayed the position and range of the TFE in a similar manner.

Discussion

In recent years, ultrasonography which results in the effective evaluation of heart structure, function, and microcirculatory changes using CEE, is widely employed in China [17]. CEE includes VO and MCE. VO can improve the image quality through heart chamber imaging and increase the accuracy of disease diagnosis. MCE is myocardial sonography that utilizes enhanced myocardial imaging to reflect myocardial and mass microcirculation and perfusion [18]. There are few reports that combine RE with CEE to diagnose EMF [19–21]. In this retrospective study, we found that such combination can make EMF diagnosis more accurate.

The ultrasound results of the sixteen EMF patients in this study were essentially the same as previously reported in the literature [4,22,23]. Each EMF subtype presented their own characteristics. RV-EMF showed an abnormally enlarged RA, a normal LA and LV size, IVC dilation, and the most severe TR. LV-EMF presented significant LA enlargement, normal or mild enlargement of the RA, and mild to moderate elevation in PASP. Bi-EMF presents bilateral atrial enlargement, an IVC collapsibility index $<$50%, and mild to moderate elevation in the PASP. We found that 69% of EMF patients had apical thrombus calcifications, which were located at the edge of the apical occlusions, next to the heart chamber, and often presenting as a band (shown in Fig. 2C). All the Bi-EMF calcifications were located in the LV. Atrioventricular valves presented varying degrees of regurgitation, likely caused by fusion of the papillary muscles into the TFE and thrombus, resulting in the valves to pull down during systole.

According to our observations, the greater the extent of the chordae tendineae fusion, the more severe the valvular regurgitation. EMF was not difficult to diagnose if these characteristics were recognized through RE. However, a diagnosis was not possible in five of the cases. There are several reasons why this could have happened. The EMF lesions are located at the apex of the heart which constitutes the nearfield of the echocardiography; it is usually difficult to clearly delineate ventricular apex structural abnormalities in RE, particularly when the operator is an inexperienced physician. When Apical calcification is severe, there is significant sound attenuation that prevents the basal chambers from being clearly displayed. Hence, excessive basal ventricular motion and heart chamber deformation cannot be observed. In addition, the echoes of TFE and thrombus in the apical region are not so different from those of myocardial tissue for early-stage EMF patients. These results tend to be overlooked or patients who are diagnosed with apical hypertrophic cardiomyopathy (APHCM).

Eleven patients underwent the CEE examination, and VO clearly showed the morphology, size, and unique "mushroom sign" of the ventricles. In the MCE, the TFE perfusion might differ from normal myocardium due to the following reasons: (1) EMF lesions can affect all layers of the myocardium, but chronic inflammatory infiltration, fibrotic changes, and neovascularization mainly occur in a thickened endomyocardium [3,24]. The composition and route of neovascularization were different from those of normal myocardial vessels, and this resulted in delayed blood perfusion of the endomyocardium compared with the normal myocardium. (2) The main coronary artery supplying blood to the myocardium from the outside is located on the surface of the heart. When the blood perfusion rate of endomyocardium is slow, a gradual perfusion enhancement from outside to inside can be observed in the MCE. The MCE showed the TFE location and extent, and it was similar to the CMR. In addition, as there was chronic inflammation in the endocardium, the surface was uneven, resulting in mural thrombus easily. There was no blood supply to the thrombus, so the uncalcified thrombus appeared dark in the plateau phase of the MCE. Because it was located at the edge of the apical occlusions, next to the heart cavity, it was poorly demarcated from the heart cavity filled with contrast medium. Hence, the MCE was far less sensitive to calcification than the RE. However, the combination of both images allowed for an easy thrombus range determination. We found that there were uncalcified thrombi below the calcified area, when calcification existed in 11 patients with EMF. The number and location of thrombus demonstrated by the MCE combined with the RE were consistent with the CMR.

The CEE can help to differentiate EMF from the following diseases: (1) APHCM: Bi-EMF and LV-EMF tend to be misdiagnosed as APHCM. APHCM cardiac imaging presents as a decreased apical chamber size, a "spade-shaped" heart chamber during diastole (Fig. 4C), apical ventricular aneurysm in some patients, and uniform myocardial perfusion. (2) Coronary heart disease with apical thrombus: EMF patients have normal apical myocardial pulsation, as the apical thrombus is fixed, it tends to be mistaken for an apical abnormal segmental wall motion in RE. CEE can easily show that the ventricular wall motion amplitude is not decreased, myocardial perfusion is normal, and there is no reduction or loss of perfusion in EMF patients to facilitate differentiation between EMF and coronary heart disease with apical thrombus. (3) Ebstein anomaly: a study [20] reported the misdiagnosis of EMF as an Ebstein anomaly. The patient underwent tricuspid valve replacement surgery, but their symptoms did not improve after surgery. Due to an insufficient understanding of EMF, the right ventricle shrinkage and the downward valve traction during systole were misdiagnosed as an Eb-

stein anomaly (Video 4). In Ebstein anomaly patients, the anterior leaflet of the tricuspid valve is long and shaped like a sail; the septal and posterior leaflet attachment sites are displaced downward; and the right ventricle is small but the apical occlusion is absent. (4) Right ventricular cardiomyopathy: this is a chronic cardiomyopathy that is limited to the right ventricular myocardium and is typically accompanied by a ventricular aneurysm. In EMF, there is excessive basal ventricular wall motion and outward bulging during diastole that tends to be mistaken for ventricular aneurysm. CEE can more clearly show the characteristics of right ventricle enlargement, wall thinning and diffuse hypokinesia in right ventricular cardiomyopathy.

In RV-EMF, compared to other EMF subtypes in this study [7], the extent of occlusion was broader; the apical thrombus calcification was more likely; significant atrial enlargement was present; and tricuspid regurgitation was more severe. This may be explained by the fact that right heart failure symptoms appeared later than left heart failure and that the apex of the RV was more difficult to clearly visualize than the apex of the LV, which resulted in diagnosis at an advanced stage. Therefore, CEE can be performed for prompt diagnosis when only right atrial enlargement is present and cannot be explained by other diseases.

Surgical intervention is the recommended treatment for patients with signs of severe ventricular restriction and NYHA functional classes III and IV [25,26]. The MCE can display anatomical details, such as the area of the TFE and thrombus. This can help in formulating preoperative surgery and postoperative follow-up plans. When calcification is absent in apical thrombus, the thrombus may fall off and embolize other organs. Hence, thrombolytic therapy might be required. It is difficult to distinguish TFE and thrombus using RE. MCE can determine whether there is a thrombus and evaluate the therapeutic effects.

Limitations of this study include the following: (1) This is a retrospective single-center study, which may increase the bias of the results. (2) The incidence of EMF in China is low. Hence, we searched case data from the past ten years, and the number of patients who could be included in the study was relatively small and even smaller after grouping. This reduced the statistical power.

Conclusions

By studying the routine echocardiograms of several EMF patients, it was found that EMF has characteristic routine echocardiography results, and the different EMF subtypes have unique routine echocardiography characteristics. Furthermore, CEE is excellent for displaying heart structure, ventricular wall motion, and tissue perfusion. A combination of routine echocardiography and CEE can decrease misdiagnosis, thereby allowing early treatment for EMF patients.

Abbreviations

EMF, endomyocardial fibrosis; TFE, thickened fibrotic endomyocardium; RE, ropacification; CMR, cardiac magnetic resonance imaging; MRI, magnetic resonance imaging; MR, mitral regurgitation; NYHA, New York Heart Association; TR, tricuspid regurgitation; LA, left atrium; LV, left ventricle; RA, right atrium; RV, right ventricle; PASP, pulmonary artery systolic pressure; IVC, inferior vena cava.

Availability of Data and Materials

The datasets used and/or analyzed during the current study are available from the corresponding author on reasonable request.

Author Contributions

PZ and BW designed the study. BW and YY performed the research. BW and YY collected and analyzed the data. BW and YY have been involved in drafting the manuscript and all authors have been involved in revising it critically for important intellectual content. All authors give final approval of the version to be published. All authors have participated sufficiently in the work to take public responsibility for appropriate portions of the content and agreed to be accountable for all aspects of the work in ensuring that questions related to its accuracy or integrity.

Ethics Approval and Consent to Participate

The study was approved by the Institutional Review Board of Guangdong Second Provincial General Hospital (approval number: 2022-KY-KZ-281-01). Written informed consents to participate in this study were provided by the participants themselves or their families.

Acknowledgment

Not applicable.

Funding

This research received no external funding.

Conflict of Interest

The authors declare no conflict of interest.

Supplementary Material

Supplementary material associated with this article can be found, in the online version, at https://doi.org/10.24976/Discov.Med.202335179.101.

References

[1] Connor DH, Somers K, Hutt MS, Manion WC, D'Arbela PG. Endomyocardial fibrosis in Uganda (Davies' disease). II. An epidemiologic, clinical, and pathologic study. American Heart Journal. 1968; 75: 107–124.

[2] Moraes F, Lapa C, Hazin S, Tenorio E, Gomes C, Moraes CR. Surgery for endomyocardial fibrosis revisited. European Journal of Cardio-Thoracic Surgery. 1999; 15: 309–312; discussion 312–313.

[3] Grimaldi A, Mocumbi AO, Freers J, Lachaud M, Mirabel M, Ferreira B, *et al*. Tropical Endomyocardial Fibrosis: Natural History, Challenges, and Perspectives. Circulation. 2016; 133: 2503–2515.

[4] Beaton A, Mocumbi AO. Diagnosis and Management of Endomyocardial Fibrosis. Cardiology Clinics. 2017; 35: 87–98.

[5] Negri F, Fabris E, Masè M, Vitrella G, Minà C, Turrisi M, *et al*. Endomyocardial fibrosis of the right ventricle: A case report of successful surgery. Journal of Cardiac Surgery. 2020; 35: 460–463.

[6] Duraes AR, de Souza Lima Bitar Y, Roever L, Neto MG. Endomyocardial fibrosis: past, present, and future. Heart Failure Reviews. 2020; 25: 725–730.

[7] de Carvalho FP, Azevedo CF. Comprehensive Assessment of Endomyocardial Fibrosis with Cardiac MRI: Morphology, Function, and Tissue Characterization. Radiographics. 2020; 40: 336–353.

[8] Perazzolo Marra M, Thiene G, Rizzo S, De Lazzari M, Carturan E, Tona F, *et al*. Cardiac magnetic resonance features of biopsy-proven endomyocardial diseases. JACC. Cardiovascular Imaging. 2014; 7: 309–312.

[9] León D, Martín M, Corros C, Santamarta E, Costilla S, Lambert JL. Usefulness of cardiac MRI in the early diagnosis of endomyocardial fibrosis. Portuguese Journal of Cardiology. 2012; 31: 401–402.

[10] Salemi VMC, Rochitte CE, Shiozaki AA, Andrade JM, Parga JR, de Ávila LF, *et al*. Late gadolinium enhancement magnetic resonance imaging in the diagnosis and prognosis of endomyocardial fibrosis patients. Circulation. Cardiovascular Imaging. 2011; 4: 304–311.

[11] Jariwala N, McGraw S, Rangarajan VS, Mirza O, Wong J, Farzaneh-Far A. The 'V' sign of endomyocardial fibrosis. QJM. 2015; 108: 423–424.

[12] Stamenkovic J, Parezanovic V, Kontic-Vucinic O, Stefanovic I, Trkulja M, Jovanovic I, *et al*. Prenatally diagnosed fetal heart rhythm abnormalities-incidence, diagnosis and outcome. Clinical and Experimental Obstetrics & Gynecology. 2022; 49: 140.

[13] Attar RH, Little SH, Faza NN. Transcatheter mitral valve repair for primary mitral regurgitation. Reviews in Cardiovascular Medicine. 2022; 23: 116.

[14] Ma N, Mou X, Yuan H, Lai Y, Jiang B. Right Sinus of Valsalva Aneurysm and Dissection into the Interventricular Septum: A Case Report. Heart Surg Forum. 2022; 30; 25: E773–E777.

[15] Lang RM, Badano LP, Mor-Avi V, Afilalo J, Armstrong A, Ernande L, *et al*. Recommendations for cardiac chamber quantification by echocardiography in adults: an update from the American Society of Echocardiography and the European Association of Cardiovascular Imaging. Journal of the American Society of Echocardiography. 2015; 28: 1–39.e14.

[16] Zoghbi WA, Adams D, Bonow RO, Enriquez-Sarano M, Foster E, Grayburn PA, *et al*. Recommendations for Noninvasive Evaluation of Native Valvular Regurgitation: A Report from the American Society of Echocardiography Developed in Collaboration with the Society for Cardiovascular Magnetic Resonance. Journal of the American Society of Echocardiography. 2017; 30: 303–371.

[17] Tian J, Ding Y, Wang Q. Left heart contrast echocardiography: development and application. Journal of Clinical Ultrasound in Medicine. 2017; 19: 838–840.

[18] Porter TR, Abdelmoneim S, Belcik JT, McCulloch ML, Mulvagh SL, Olson JJ, *et al*. Guidelines for the cardiac sonographer in the performance of contrast echocardiography: a focused update from the American Society of Echocardiography. Journal of the American Society of Echocardiography. 2014; 27: 797–810.

[19] Rassi DDC, Marçal PC, Cruz CBBV, Masson Silva JB, Hotta VT. Multimodality Imaging in Endomyocardial Fibrosis: Diagnosis and Assessment of the Extent of the Disease. Circulation. Cardiovascular Imaging. 2021; 14: e012093.

[20] Oh J, Kim SH, Youn JC, Choi BW, Kang SM. Endomyocardial fibrosis: evaluation with myocardial contrast echocardiography and magnetic resonance imaging. The Canadian Journal of Cardiology. 2012; 28: 612.e11–612.e12.

[21] Sutter JS, Suboc TM, Rao AK. Tropical Endomyocardial Fibrosis. JACC. Case Reports. 2020; 2: 819–822.

[22] Berensztein CS, Piñeiro D, Marcotegui M, Brunoldi R, Blanco MV, Lerman J. Usefulness of echocardiography and doppler echocardiography in endomyocardial fibrosis. Journal of the American Society of Echocardiography. 2000; 13: 385–392.

[23] Hassan WM, Fawzy ME, Al Helaly S, Hegazy H, Malik S. Pitfalls in diagnosis and clinical, echocardiographic, and hemodynamic findings in endomyocardial fibrosis: a 25-year experience. Chest. 2005; 128: 3985–3992.

[24] Mocumbi AO, Yacoub S, Yacoub MH. Neglected tropical cardiomyopathies: II. Endomyocardial fibrosis: myocardial disease. Heart. 2008; 94: 384–390.

[25] Yangni-Angate KH, Meneas C, Diby F, Diomande M, Adoubi A, Tanauh Y. Cardiac surgery in Africa: a thirty-five year experience on open heart surgery in Cote d'Ivoire. Cardiovascular Diagnosis and Therapy. 2016; 6: S44–S63.

[26] Mocumbi AO, Stothard JR, Correia-de-Sá P, Yacoub M. Endomyocardial Fibrosis: an Update After 70 Years. Current Cardiology Reports. 2019; 21: 148.